Profile and Molecular Modeling of 3-(Indole-3-yl)-4-(3,4,5-trimethoxyphenyl)-1*H*-pyrrole-2,5-dione (1) as a Highly Selective VEGF-R2/3 Inhibitor

Christian Peifer,*,[†] Agata Krasowski,[†] Nina Hämmerle,[†] Oliver Kohlbacher,[‡] Gerd Dannhardt,[§] Frank Totzke,[#] Christoph Schächtele,[#] and Stefan Laufer[†]

Department of Pharmacy, Eberhard Karls University, Auf der Morgenstelle 8, D-72076 Tübingen, Germany, Center for Bioinformatics, Eberhard Karls University, Sand 14, D-72076 Tübingen, Germany, Department of Pharmacy, Johannes Gutenberg University, Staudingerweg 5, D-55099 Mainz, Germany, and ProQinase GmbH, Breisacherstrasse 117, D-79106 Freiburg, Germany

We report on selectivity profiling of **1** in a panel of 20 protein kinases and molecular modeling indicating **1** to be highly active and selective for VEGF-R2/3. Sequence alignment analysis and detailed insights into the ATP binding pockets of targeted protein kinases from the panel result in a unique structural architecture of VEGF-R2 mainly caused by the hydrophobic pocket I, determining the molecular basis for activity and selectivity of **1**.

Introduction

Protein kinases (PKs) comprise 22% of the druggable genome and are currently among the most important and promising target classes for drug discovery.[1] PKs regulate signal transduction by phosphorylating tyrosine, threonine, and serine residues in key proteins involved in signal pathways with significant relevance to many diseases. Thus, small-molecule inhibitors of these pathways can be used to treat diseases such as cancer,[2] diabetes, and inflammation.[3,4] Since all 518 PKs of the kinome use ATP as a cofactor to carry out the phosphorylation of specific signal proteins, they share a highly conserved ATP binding pocket that serves as the molecular binding site of most inhibitors.[5] To make things even more complex, there are different expression levels of hundreds of PKs and cell signaling proteins in different organs. Furthermore, the phosphorylation status depends on complex physiological and pathophysiological situations in patients.[6] Thus, for drug candidates that interfere with PKs, it is essential to have an understanding of the structural basis for selectivity and specifity within the kinome (and beyond[7]) and a method for the robust evaluation of potency and selectivity.[8,9] Currently, there is no consensus whether the concepts of single-targeting, group-targeting, multitargeting, or even promiscous inhibitors across kinase space may result in potential therapeutical benefits.[10,11] To extensively address the topic of kinase selectivity of a preclinical compound, it would be optimal to screen and characterize its activity against all 518 PKs of the kinome. However, an appropriate approach in early drug discovery would be to evaluate potency against a significant panel of selected members of PK families[12] and to evaluate its activity in cellular assays.[10] Clinical data will ultimately tell us if custom-made or promiscous inhibitors of PKs can provide therapeutic benefits.[13] Most research activities regarding the development of small-molecule inhibitors of PKs address cancer-related tyrosine kinases (TK),[14] and to date, six ATP-competitive small-molecule inhibitors with very different selectivity profiles have been approved as anticancer drugs (Table 1).

In addition, many PK inhibitors are currently in preclinical development and in clinical trials, mainly as inhibitors for cancer-relevant kinases.[14] Tyrosine kinases,[21] including vascular endothelial growth factor receptor (VEGF-R[a]) 2/3, are known to play an important role in oncology and are useful in the development of clinicaly effective inhibitors. Therefore, inhibitors of the tyrosine group of PKs are the focus of vibrant research activities.[22,23]

In our recent study, **1** (Figure 1), with remarkable antiangio-

Figure 1. Structures of **1**, **2**, and staurosporine.

genic activity, was discovered from a small set of 2,3-diarylmaleimide derivatives tested in the in vivo chick embryo assay.[24,25] To specify the molecular target, **1** was initially screened in a panel of 12 selected protein kinases and was consequently found to have an IC_{50} of 2.5 nM for the angiogenic key kinase VEGF-R2[26] and therefore determined to be a highly potent VEGF-R2 tyrosine kinase inhibitor.[25] Because this approach revealed the molecular target for **1** but with no detailed information about kinase selectivity, we were interested in investigating the inhibitory profile of **1** with respect to other kinases.
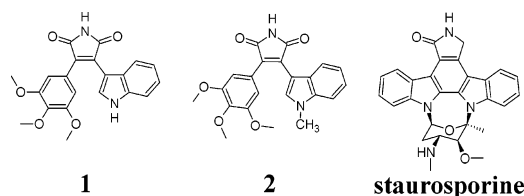
Selectivity Profiling of 1

Here, we report on selectivity profiling of **1** in a panel of 20 therapeutically relevant PKs of different families of the kinome (Figure 2) and molecular modeling studies indicating **1** to be highly active and selective for VEGF-R2 and VEGF-R3. The PKs have been selected for the determination of an IC_{50} profile of **1** because they are involved in malignant diseases and because they represent different PK families. As can be seen in Table 2, **1** is actually selective over the homologous TKs including EGF-R, ERbB2,[27] TIE2,[28] PDGFR*β*,[29] SRC,[30] and FAK.[31,32]

---

* To whom correspondence should be addressed. Phone: 0049 7071 29 75278. Fax: 0049 7071 29 5037. E-mail: Christian.Peifer@uni-tuebingen.de.
[†] Department of Pharmacy, Eberhard Karls University.
[‡] Center for Bioinformatics, Eberhard Karls University.
[§] Johannes Gutenberg University.
[#] ProQinase GmbH.

[a] Abbreviations: VEGF-R, vascular endothelial growth factor receptor; EGFR, epidermal growth factor receptor; BCR-ABL, chromosomes encoding the kinase; c-KIT, protooncogene encoding KIT (a TK receptor for the mast cell growth factor); mPDGFR-*β*, platelet derived growth factor receptor; FLt3, FMS-like receptor tyrosine kinase 3; p38α MAPK, mitogen activated PK; SRC, family of protooncogenes encoding nonreceptor tyrosine kinases; EPHA2, ephrin receptor A2.

Table 1. Protein Kinase Inhibitors Currently Approved as Drugs, Their Predominantly Target Kinases, and Their Clinical Use

Drug	Structure	Year launched	Predominantly target kinase(s) inhibited at nM concentrations	Clinical use
Imatinib mesylate/ STI571 [15]		2001	BCR-ABL, c-KIT	Chronic myelogenous leukemia (CML), gastrointestinal stromal tumors (GISTs) and a number of other malignancies. Early clinical trials also show potential for treatment of hypereosinophilic syndrome and dermatofibrosarcoma protuberans.
Gefitinib/ ZD1839 [16]		2003	EGFR	Locally advanced or metastatic non-small cell lung cancer (NSCLC) in patients who have previously received chemotherapy.
Erlotinib HCl/ OSI-774/ CP-358,774 [17]		2004	EGFR	In combination with gemcitabine for treatment of locally advanced, unresectable, or metastatic pancreatic cancer.
Sorafenib/ Bay 43-9006 [18]		2005	c-Raf/b-Raf, VEGF-R 2/3, mPDGFR-ß, Flt3 and p38αMAPK	Advanced renal cell cancer.
Sunitinib/ SU11248 [19]		2006	Multiple tyrosine receptor kinases, including PDGF-R and VEGF-R.	GIST and renal cell carcinoma (RCC). Its efficacy in GIST is due to inhibition of the mutationally active c-KIT kinase, including mutants that have become resistant to imatinib.
Dasatinib/ BMS-354825 [20]		2006	Multiple tyrosine receptor kinases including BCR-ABL, SRC family (SRC, LCK, YES, FYN), c-KIT, EPHA2, PDGFRβ	CML

Table 2. IC_{50} Values (M) of **1** in a Panel of 20 Kinase Assays

assay	IC_{50} (M)	assay	IC_{50} (M)	assay	IC_{50} (M)
EPHB4	1.6×10^{-5}	TIE2	2.8×10^{-6}	GSK3-β	1.1×10^{-6}
IGF1-R	9.9×10^{-6}	ABL1	9.3×10^{-5}	NEK2	$>1 \times 10^{-4}$
SRC	2.0×10^{-5}	INS-R	2.3×10^{-5}	FAK	9.7×10^{-7}
VEGF-R2	2.5×10^{-9}	PLK1	$>1 \times 10^{-4}$	AKT1	$>1 \times 10^{-4}$
VEGF-R3	5.0×10^{-9}	PDGFR-β	6.8×10^{-7}	Aurora-A	9.9×10^{-6}
EGF-R	3.2×10^{-5}	CDK2/CycA	8.2×10^{-6}	Aurora-B	2.5×10^{-5}
ERbB2	5.0×10^{-5}	CDK4/CycD1	9.9×10^{-6}		

Compound **1** inhibited VEGF-R2/3 in the low nanomolar range, but compared to VEGF-R2, the kinases PDGFRβ inhibited in an almost 300-fold higher concentration ($IC_{50} = 6.8 \times 10^{-7}$ M), FAK ($IC_{50} = 9.7 \times 10^{-7}$ M) and the other PKs (EPHB4,[33] IGF1-R,[34] ABL1,[35] INS-R,[36] PLK1,[37] CDK2/4,[38] GSK3-β,[39] NEK2,[40] Aurora A/B[41]) in only the micromolar range. In particular, the selectivity of **1** for VEGF-R2/3 over INS-R is important because a critical requirement for a PK inhibitor to be further developed is to avoid disturbing glucose homeostasis.[36] However, for an optimal characterization of this class of

Figure 2. Panel of 20 therapeutically relevant PKs of the kinome for selectivity profiling of **1**. Key targets VEGF-R2/3 are highlighted. The phylogenetic tree of kinases (kinome) was adapted from the literature.[5]

compounds in the kinome space, the selectivity profile needs to be expanded.

Binding mode of 1 in VEGF-R2

Molecular modeling studies revealed an interesting and reasonable binding mode of **1** in the ATP pocket of VEGF-R2, which fully explains the in vitro selectivity for VEGF-R2 over the other PKs. In detail, hydrogen bonds to the hinge backbone carbonyl of Glu915 and to the backbone amine of Cys917 are formed. The indole ring is located in the hydrophobic region I with $\pi-\pi$ stacking interactions to Phe1045, whereas the trimethoxyphenyl moiety is situated in the hydrophobic region II. No direct hydrogen bond acceptor within a radius of 4 Å of the indole−NH could be found in the protein structure.

However, SAR (in vitro VEGF-R2 assay) revealed that the free indole NH in **1** as optimal and methylation (**2**, Figure 1) decreased activity 100-fold, indicating an important ligand−protein interaction for the NH moiety.[25] Since this is the only detail in the modeled binding mode that is in conflict with the SAR data, we postulate that a water molecule can perhaps mediate NH−protein hydrogen bonding that is not detected by the docking experiments (Figure 3). First, one can argue that the sugar pocket consisting of Arg1030 and Asn1031 is located within the 6 Å distance required for water-mediated interactions and is therefore available to accept H-bonds. Second, the $\pi-\pi$ stacking interactions of **1** to Phe1045 position the indole moiety in such a way that the indole−NH points in a geometrically convenient direction toward the sugar pocket. Third, this exposed area of the ATP binding pocket is supposed to be accessible to water molecules. Furthermore, the effect of water molecules on ligand binding interactions in the ATP pocket of the cyclin-dependent kinase 2 (CDK2) was found to be pivotal.[42] The water hypothesis in this study was examined using the program GRID by calculating preferred water H-bond interaction spots toward the ATP binding site of VEGF-R2. Indeed, between Arg1030, Asn1031 and the position of indole NH, a
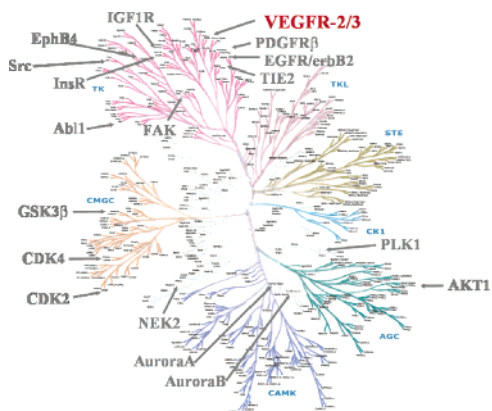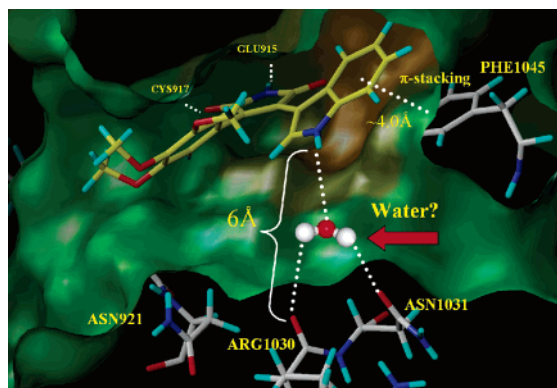
Figure 3. Crystallographically determined ATP binding site of VEGF-R2 (PDB code 1y6a) and modeled binding mode of **1** (yellow). Key residues and hydrogen bonds are labeled. For clarity, the water molecule is shown in a hypothetical position. The working hypothesis of water-mediated ligand−protein interactions was subsequently investigated by methods of molecular modeling.
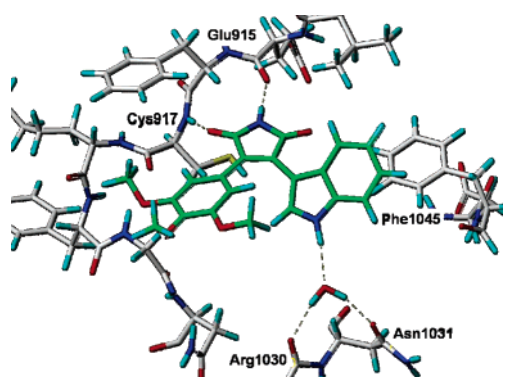

Figure 4. Crystallographically determined ATP binding site of VEGF-R2 (PDB code 1Y6A). Binding mode of **1** (green) was modeled and minimized involving a flexible complex of one molecule of water, **1**, and Glu915/Cys917/Arg1031/Asn1031. Key residues and hydrogen bonds are labeled.

favorable water location was found. On the basis of the calculated location, we placed the virtual water molecule and subsequently minimized a flexible complex of Arg1030/Asn1031/water and **1**, maintaining the H-bonds to Glu915 and Cys917. This approach revealed an expedient involvement of water in the binding mode (Figure 4) with water/carbonyl−Arg1030 = 2.14 Å, water/carbonyl−Asn1031 = 1.92 Å, and water/NH−**1** = 2.12 Å.

Binding mode of 1 in FAK

Having determined a possible binding mode for **1** in VEGF-R2, which is supported by SAR data of the compound for this enzyme, we were particularly interested in the issue of selectivity over the other protein kinases. Since **1** is structurally related to the unselective "pankinase" inhibitor staurosporine[9] (Figure 1), we investigated whether the binding modes of **1** in VEGF-R2 and other TKs account for the unexpected selectivity profile. To address this, the binding mode of **1** in VEGF-R2 (PDB code 1y6a)[43] was compared to docking results of **1** in FAK. We used the ATP pocket of FAK (PDB code 1MP8[44] (IC$_{50}$(**1**) = 1 μM) for the docking experiments since there is no crystallographically based protein structure published for PDGFRβ (IC$_{50}$(**1**) = 680 nM).

Thus, a binding mode of **1** in the ATP binding site of tyrosine kinase FAK was modeled (Figure 5). Comparable to the binding mode in VEGF-R2, hydrogen bonds to the hinge backbone carbonyl of Glu500 and to the backbone amine of Cys502 are
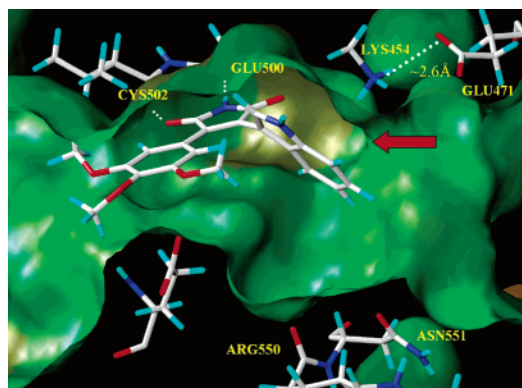

Figure 5. Crystallographically determined ATP binding site of FAK (PDB code 1MP8) and modeled binding mode of **1** (white). Key residues and hydrogen bonds are labeled. Compared to the ATP pocket of VEGF-R2, hydrophobic region I in FAK is less spacious (indicated by red arrow), causing a twisted and suboptimal binding of the indole moiety.

Figure 6. Sequence alignment of ATP binding pocket areas of targeted PKs (with PDB code and name) for key residues in VEGF-R2, (F) Phe1045 in a DFGL motif, and (R) Arg1030/(N) Asn1031 in an ARN motif. Positions in TKs are as follows: SRC (F)333 (N)319; FAK (F)-565 (N)551; EGFR (F)856 (N)842; ABL1 (F)382 (N)368. Positions in AGC kinase (containing PKA, PKG, PKC families) are Aurora-B (F)-235 (N)221. Positions in CMGC kinases (containing CDK, MAPK, GSK3, CLK families) are CDK2 (F)146 (N)132, GSK3 (F)201 (N)-187.

formed and the trimethoxyphenyl moiety is situated in hydrophobic region II. But significantly different from the ATP binding site of VEGF-R2, in FAK the indole moiety of **1** is twisted out of the minor hydrophobic region I, presumably forming a cation−π stacking with protonated Lys454 (which itself is fixed by a salt bridge with Glu471). Taken together, because of the small dimensions of hydrophobic region I and the resulting suboptimal orientation of the indole moiety in FAK, the key water-mediated hydrogen bond to the sugar pocket (Arg550/Asn551) is prevented. This binding mode is in accordance with an almost 400-fold loss of activity for **1** in the FAK assay compared to VEGF-R2.

Even if accurate and realistic in silico docking remains a challenge, the binding modes of **1** in VEGF-R2 and FAK are consistent with SAR in the in vitro selectivity profile and can serve as rational models explaining the high activity for VEGF-R2 and the selectivity over FAK. As mentioned above, in this binding mode, residue Phe1045 of hydrophobic pocket I in VEGF-R2 is key, fixing the indole moiety into a water-mediated interaction to Arg1030/Asn1031, accounting for high activity and selectivity of **1** in VEGF-R2. To evaluate the position of the conserved Phe in the other PKs of the panel, we aligned the sequences of the targeted PKs for which PDB structures were published (Figure 6).

Furthermore, by overlaying the backbone of the ATP binding pocket of VEGF-R2 with targeted PKs of the panel (for which PDB structures were published), we examined the orientation of Phe and Asn (key residues in the binding mode of **1** in VEGF-R2) in each of the kinases (Figure 7). Although highly conserved in all these PK sequences, the Phe residue can be found in quite
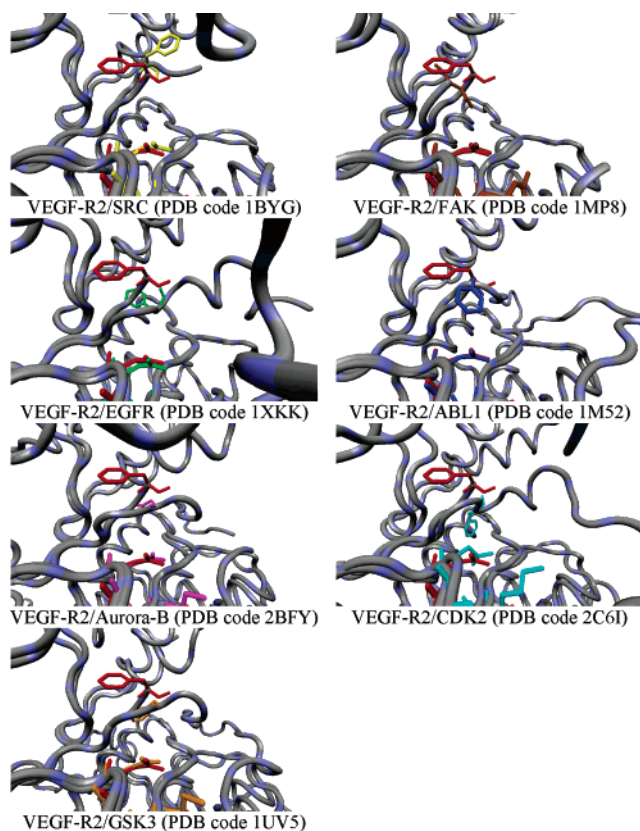
Figure 7. Backbone overlay of ATP binding pocket areas of VEGF-R2 with targeted PKs (PDB structures). Conserved key residues Phe1045 and Asn1031 in VEGF-R2 are maintained in red and colored differently in each case. For FAK, the position of Phe565 is not exactly defined in the PDB structure, and therefore, immediate neighbor residue Asp564 is highlighted.

VEGF-R2   KCIHRDLA**ARN**ILLSEKNVV-KIC**DFGL**ARDIYKDPDYVRKGDARL
VEGF-R3   KCIHRDLA**ARN**ILLSESDVVKIC**DFGL**ARDIYKDPDYVRKGSARL

Figure 8. Sequence analogy of highly homologous ATP binding pocket areas of VEGF-R2 and VEGF-R3. Key residues in VEGF-R2 are as follows: (F) Phe1045 and (R) Arg1030/(N) Asn1031. Key residues in VEGF-R3 are as follows: (F) Phe1056 and (R) Arg1041/(N) Asn1042.

different orientations whereas residue Asn remains in almost the same position, as indicated in Figure 7. However, in VEGF-R2 only, Phe1045 is situated in a suitable position for the indole moiety to make water-mediated interaction, as discussed in the binding mode. Thus, in combination with the other ligand−protein interactions, Phe1045 especially provides the molecular basis for activity and selectivity of **1** in this important drug target. Finally, X-ray crystallographic data of a ligand−protein complex will confirm the modeled binding mode in this study.

Compound **1** was also found to be active for VEGF-R3 in the low nanomolar range (IC_{50} = 5 nM), but no crystal structure was published to perform modeling experiments at the ATP binding site of this kinase. Sequence comparison of VEGF-R2/VEGF-R3 (Figure 8) shows significant homology, and therefore, the orientation of Phe and Asn can be considered to be comparable between these kinases, resulting in a comparable binding mode in VEGF-R3 for **1**.

Pharmacological and Clinical Relevance of VEGF-R Inhibitors

In light of the biological role of VEGF-R2 as an essential factor for the function of endothelial cells and VEGF-R3 for lymphendothelial cells,[45] the inhibition of both kinases can result in a strong antiangiogenic effect. However, because of the

conserved architecture of the ATP binding pocket, it is unlikely that an ATP-competitive compound with high activity against a single PK will leave the other 517 PKs unaffected. Potent VEGF-R inhibitors such as SU5416, SU6668, PTK787, ZK-222584, CGP-79787(D), CP-547632, and AZD2171 have been developed with different in vitro selectivities but "reasonable side effect profiles" and with in vivo efficacy.[46] Furthermore, approved multikinase inhibitors like sunitinib and vatalanib are also highly active inhibitors of VEGF-R2, and the potent orally active VEGF-R2 inhibitor ZD6474/vandetanib with inhibitory activity for EGF-R and RET kinase is currently in clinical development.[47] Therefore, **1** can be useful as a pharmacological tool for inhibiting VEGF-R2/R3 in signal transduction studies and a reference compound in in vivo angiogenesis assays.[24] Considering the high in vitro potency and selectivity for VEGF-R2/3, as well as being bioavailable in the chick embryo model,[25] **1** may have potential for development as a potent and selective VEGF-R2/3 inhibitor in angiogenic-relevant diseases. However, an enhanced selectivity profile in the kinome space and evaluation in further in vivo angiogenic models are underway to characterize the preclinical potential of **1**. Even though **1** shows promising in vitro efficiency with selectivity for VEGF-R2/3, future studies will answer the question if selective or promiscuous PK inhibitors can result in clinical benefits.

Experimental Section

Chemistry. Compounds **1** and **2** were synthesized by one-pot condensation of 3,4,5-trimethoxyphenylacetamide with (indolyl-3)-ethylglyoxylate for **1** and ethyl-(1-methylindol-3-yl)-glyoxylate for **2** using KOBu*t* and 4 Å molecular sieves in THF.[25]

Molecular Modeling. The modeling for **1** was performed on a Fedora Core 3 Linux system. For visualization and building the structures, Sybyl 7.1 (Tripos Inc., St. Louis, MO) was used. The Connolly surface was calculated using the MOLCAD module in Sybyl and colored according to lipophilicity (from very hydrophobic to hydrophilic, corresponding to brown to green to blue). The active site in VEGF-R2 and FAK was defined as 6.5 Å surrounding the ligand. Compound **1** was docked into the active site of VEGF-R2 and FAK using the FlexX docking program.[48] The FlexX scoring function was applied during the placement and construction phase of the ligands, and DrugScore was used for the final ranking.[49] The 3D coordinates of the VEGF-R2 catalytic core in complex with a 2-anilino-5-aryloxazole inhibitor were taken from the Brookhaven Protein Databank (PDB code: 1Y6A). The 3D coordinates of the FAK catalytic core in complex with ligand adenosine 5′-diphosphate were taken from the Brookhaven Protein Databank (PDB code: 1MP8).

Favorable water interaction regions in the ATP binding pocket of VEGF-R2 (PDB code: 1Y6A) were calculated using the program GRID 2a (2004).[50] Between Arg1030, Asn1031, and the position of the indole NH, a water spot was found with a minimum interaction energy of −6.113 kcal/mol.

The overlay and visualization of structures were performed with BALLView,[51] version 1.1.1 (07.01.2006) using the 3D coordinates of the Brookhaven Protein Databank PDB structures 1Y6B (VEGF-R2), 1BYG (SRC), 1MP8 (FAK), 1XKK (EGFR), 1M52 (ABL1), 2BFY (AUR-B), 2C6I (CDK2), 1UV5 (GSK3).

Supporting Information Available: Results of **1** (at 10 μM) in an initial screening panel of 12 kinase assays and experimental section for selectivity profiling **1** using 20 kinases by IC_{50} values. This material is available free of charge via the Internet at http://pubs.acs.org.

References

(1) Hopkins, A. L.; Groom, C. R. The druggable genome. *Nat. Rev. Drug Discovery* **2002**, *1*, 727−730.

(2) Blume-Jensen, P.; Hunter, T. Oncogenic kinase signalling. *Nature* **2001**, *411*, 355−365.

(3) Shawver, L. K.; Slamon, D.; Ullrich, A. Smart drugs: tyrosine kinase inhibitors in cancer therapy. *Cancer Cell* **2002**, *1*, 117−123.

(4) Kung, C.; Shokat, K. M. Small-molecule kinase−inhibitor target assessment. *ChemBioChem* **2005**, *6*, 523−526.

(5) Manning, G.; Whyte, D. B.; Martinez, R.; Hunter, T.; Sudarsanam, S. The protein kinase complement of the human genome. *Science* **2002**, *298*, 1912−1916, 1933.

(6) Daub, H. Characterisation of kinase-selective inhibitors by chemical proteomics. *BBA−Proteins Proteomics* **2005**, *1754*, 183−190.

(7) McGovern, S. L.; Shoichet, B. K. Kinase inhibitors: Not just for kinases anymore. *J. Med. Chem.* **2003**, *46*, 1478−1483.

(8) Luo, Y. Selectivity assessment of kinase inhibitors: Strategies and challenges. *Curr. Opin. Mol. Ther.* **2005**, *7*, 251−255.

(9) Fabian, M. A.; Biggs, W. H., III; Treiber, D. K.; Atteridge, C. E.; Azimioara, M. D.; Benedetti, M. G.; Carter, T. A.; Ciceri, P.; Edeen, P. T.; Floyd, M.; Ford, J. M.; Galvin, M.; Gerlach, J. L.; Grotzfeld, R. M.; Herrgard, S.; Insko, D. E.; Insko, M. A.; Lai, A. G.; Lias, J. M.; Mehta, S. A.; Milanov, Z. V.; Velasco, A. M.; Wodicka, L. M.; Patel, H. K.; Zarrinkar, P. P.; Lockhart, D. J. A small molecule−kinase interaction map for clinical kinase inhibitors. *Nat. Biotechnol.* **2005**, *23*, 329−336.

(10) Knight, Z. A.; Shokat, K. M. Features of selective kinase inhibitors. *Chem. Biol.* **2005**, *12*, 621−637.

(11) Kung, C.; Kenski, D. M.; Krukenberg, K.; Madhani, H. D.; Shokat, K. M. Selective kinase inhibition by exploiting differential pathway sensitivity. *Chem. Biol.* **2006**, *13*, 399−407.

(12) Horiuchi, K. Y.; Wang, Y.; Diamond, S. L.; Ma, H. Microarrays for the functional analysis of the chemical-kinase interactome. *J. Biomol. Screening* **2006**, *11*, 48−56.

(13) Zhang, Z.; Meier, K. E. New assignments for multitasking signal transduction inhibitors. *Mol. Pharmacol.* **2006**, *69*, 1510−1512.

(14) Vieth, M.; Sutherland, J. J.; Robertson, D. H.; Campbell, R. M. Kinomics: Characterizing the therapeutically validated kinase space. *Drug Discovery Today* **2005**, *10*, 839−846.

(15) Capdeville, R.; Buchdunger, E.; Zimmermann, J.; Matter, A. Glivec (STI571, imatinib), a rationally developed, targeted anticancer drug. *Nat. Rev. Drug Discovery* **2002**, *1*, 493−502.

(16) Cappuzzo, F.; Finocchiaro, G.; Metro, G.; Bartolini, S.; Magrini, E.; Cancellieri, A.; Trisolini, R.; Castaldini, L.; Tallini, G.; Crino, L. Clinical experience with gefitinib: An update. *CRC Crit. Rev. Oncol.-Hematol.* **2006**, *58*, 31−45.

(17) Leighl, N. B.; Res, D. Erlotinib: Profile report. *Drugs Ther. Perspect.* **2006**, *22*, 1−2.

(18) Rini, B. I. Sorafenib. *Expert Opin. Pharmacother.* **2006**, *7*, 453−461.

(19) Atkins, M.; Jones, C. A.; Kirkpatrick, P. Sunitinib maleate. *Nat. Rev. Drug Discovery* **2006**, *5*, 279−280.

(20) McIntyre, J. A.; Er, J.; Bayes, M. Dasatinib. Treatment of leukemia treatment of solid tumors Bcr-Abl and Src kinase inhibitor. *Drugs Future* **2006**, *31*, 291−303.

(21) Grosios, K.; Traxler, P. Tyrosine kinase targets in drug discovery. *Drugs Future* **2003**, *28*, 679−697.

(22) Arora, A.; Scholar, E. M. Role of tyrosine kinase inhibitors in cancer therapy. *J. Pharmacol. Exp. Ther.* **2005**, *315*, 971−979.

(23) Krause, D. S.; Van Etten, R. A. Tyrosine kinases as targets for cancer therapy. *New Engl. J. Med.* **2005**, *353*, 172−187.

(24) Peifer, C.; Dannhardt, G. A novel quantitative chick embryo assay as an angiogenesis model using digital image analysis. *Anticancer Res.* **2004**, *24*, 1545−1551.

(25) (a) Peifer, C.; Stoiber, T.; Unger, E.; Totzke, F.; Schächtele, C.; Marmé, D.; Brenk, R.; Klebe, G.; Schollmeyer, D.; Dannhardt, G. Design, synthesis, and biological evaluation of 3,4-diarylmaleimides as angiogenesis inhibitors. *J. Med. Chem.* **2006**, *49*, 1271−1281. (b) Dannhardt, G. and Peifer, C. 3-(Indolyl)-4-arylmaleimide derivatives and their use as angiogenesis inhibitors. Patent WO 2006/061212 A1, 2006.

(26) Boyer, S. J. Small molecule inhibitors of KDR (VEGFR-2) kinase: an overview of structure activity relationships. *Curr. Top. Med. Chem.* **2002**, *2*, 973−1000.

(27) Kane, S. E. Cancer therapies targeted to the epidermal growth factor receptor and its family members. *Expert Opin. Ther. Pat.* **2006**, *16*, 147−164.

(28) Miyazaki, Y.; Matsunaga, S.; Tang, J.; Maeda, Y.; Nakano, M.; Philippe, R. J.; Shibahara, M.; Liu, W.; Sato, H.; Wang, L.; Nolte, R. T. Novel 4-amino-furo[2,3-*d*]pyrimidines as Tie-2 and VEGFR2 dual inhibitors. *Bioorg. Med. Chem. Lett.* **2005**, *15*, 2203−2207.

(29) Roberts, W. G.; Whalen, P. M.; Soderstrom, E.; Moraski, G.; Lyssikatos, J. P.; Wang, H. F.; Cooper, B.; Baker, D. A.; Savage, D.; Dalvie, D.; Atherton, J. A.; Ralston, S.; Szewc, R.; Kath, J. C.; Lin, J.; Soderstrom, C.; Tkalcevic, G.; Cohen, B. D.; Pollack, V.; Barth, W.; Hungerford, W.; Ung, E. Antiangiogenic and antitumor activity of a selective PDGFR tyrosine kinase inhibitor, CP-673,-451. *Cancer Res.* **2005**, *65*, 957−966.

(30) Chen, T.; Georgea, J. A.; Taylor, C. C. Src tyrosine kinase as a chemotherapeutic target: Is there a clinical case? *Anti-Cancer Drugs* **2006**, *17*, 123−131.

(31) Choi, H. S.; Wang, Z.; Richmond, W.; He, X.; Yang, K.; Jiang, T.; Karanewsky, D.; Gu, X.; Zhou, V.; Liu, Y.; Che, J.; Lee, C. C.; Caldwell, J.; Kanazawa, T.; Umemura, I.; Matsuura, N.; Ohmori, O.; Honda, T.; Gray, N.; He, Y. Design and synthesis of 7*H*-pyrrolo-[2,3-*d*]pyrimidines as focal adhesion kinase inhibitors. Part 2. *Bioorg. Med. Chem. Lett.* **2006**, *16*, 2689−2692.

(32) Choi, H. S.; Wang, Z.; Richmond, W.; He, X.; Yang, K.; Jiang, T.; Sim, T.; Karanewsky, D.; Gu, X. J.; Zhou, V.; Liu, Y.; Ohmori, O.; Caldwell, J.; Gray, N.; He, Y. Design and synthesis of 7*H*-pyrrolo-[2,3-*d*]pyrimidines as focal adhesion kinase inhibitors. Part 1. *Bioorg. Med. Chem. Lett.* **2006**, *16*, 2173−2176.

(33) Brantley-Sieders, D. M.; Chen, J. Eph receptor tyrosine kinases in angiogenesis: From development to disease. *Angiogenesis* **2004**, *7*, 17−28.

(34) Menu, E.; Jernberg-Wiklund, H.; Stromberg, T.; De Raeve, H.; Girnita, L.; Larsson, O.; Axelson, M.; Asosingh, K.; Nilsson, K.; Van Camp, B.; Vanderkerken, K. Inhibiting the IGF-1 receptor tyrosine kinase with the cyclolignan PPP: An in vitro and in vivo study in the 5T33MM mouse model. *Blood* **2006**, *107*, 655−660.

(35) Wong, S.; Witte, O. N. The BCR-ABL story: Bench to bedside and back. *Annu. Rev. Immunol.* **2004**, *22*, 247−306.

(36) Yee, D. Targeting insulin-like growth factor pathways. *Br. J. Cancer* **2006**, *94*, 465−468.

(37) McInnes, C.; Mezna, M.; Fischer, P. M. Progress in the discovery of Polo-like kinase inhibitors. *Curr. Top. Med. Chem.* **2005**, *5*, 181−197.

(38) Blagden, S.; de Bono, J. Drugging cell cycle kinases in cancer therapy. *Curr. Drug Targets* **2005**, *6*, 325−335.

(39) Smalley, J.; Peat, A. J.; Boucheron, J. A.; Dickerson, S.; Garrido, D.; Preugschat, F.; Schweiker, S. L.; Thomson, S. A.; Wang, T. Y. Synthesis and evaluation of novel heterocyclic inhibitors of GSK-3. *Bioorg. Med. Chem. Lett.* **2006**, *16*, 2091−2094.

(40) Hayward, D. G.; Clarke, R. B.; Faragher, A. J.; Pillai, M. R.; Hagan, I. M.; Fry, A. M. The centrosomal kinase Nek2 displays elevated levels of protein expression in human breast cancer. *Cancer Res.* **2004**, *64*, 7370−7376.

(41) Matthews, N.; Visintin, C.; Hartzoulakis, B.; Jarvis, A.; Selwood, D. L. Aurora A and B kinases as targets for cancer: Will they be selective for tumors? *Expert Rev. Anticancer Ther.* **2006**, *6*, 109−120.

(42) Garcia-Sosa, A. T.; Mancera, R. L. The effect of a tightly bound water molecule on scaffold diversity in the computer-aided de novo ligand design of CDK2 inhibitors. *J. Mol. Model.* **2006**, *12*, 422−431.

(43) Harris, P. A.; Cheung, M.; Hunter, R. N., III; Brown, M. L.; Veal, J. M.; Nolte, R. T.; Wang, L.; Liu, W.; Crosby, R. M.; Johnson, J. H.; Epperly, A. H.; Kumar, R.; Luttrell, D. K.; Stafford, J. A. Discovery and evaluation of 2-anilino-5-aryloxazoles as a novel class of VEGFR2 kinase inhibitors. *J. Med. Chem.* **2005**, *48*, 1610−1619.

(44) Nowakowski, J.; Cronin, C. N.; McRee, D. E.; Knuth, M. W.; Nelson, C. G.; Pavletich, N. P.; Rogers, J.; Sang, B. C.; Scheibe, D. N.; Swanson, R. V.; Thompson, D. A. Structures of the cancer-related Aurora-A, FAK, and EphA2 protein kinases from nanovolume crystallography. *Structure* **2002**, *10*, 1659−1667.

(45) Olsson, A. K.; Dimberg, A.; Kreuger, J.; Claesson-Welsh, L. VEGF receptor signalling−in control of vascular function. *Nat. Rev. Mol. Cell Biol.* **2006**, *7*, 359−371.

(46) Wiedmann, M. W.; Caca, K. Molecularly targeted therapy for gastrointestinal cancer. *Curr. Cancer Drug Targets* **2005**, *5*, 171−193.

(47) Zareba, G.; Castaner, J.; Bozzo, J. Vandetanib. Angiogenesis inhibitor VEGFR inhibitor. *Drugs Future* **2005**, *30*, 138−145.

(48) Rarey, M.; Kramer, B.; Lengauer, T.; Klebe, G. A fast flexible docking method using an incremental construction algorithm. *J. Mol. Biol.* **1996**, *261*, 470−489.

(49) Gohlke, H.; Hendlich, M.; Klebe, G. Knowledge-based scoring function to predict protein−ligand interactions. *J. Mol. Biol.* **2000**, *295*, 337−356.

(50) Goodford, P. J. A computational procedure for determining energetically favorable binding sites on biologically important macromolecules. *J. Med. Chem.* **1985**, *28*, 849−857.

(51) Moll, A.; Hildebrandt, A.; Lenhof, H. P.; Kohlbacher, O. BALL-View: An object-oriented molecular visualization and modeling framework. *J. Comput.-Aided Mol. Des.* **2005**, *19*, 791−800.